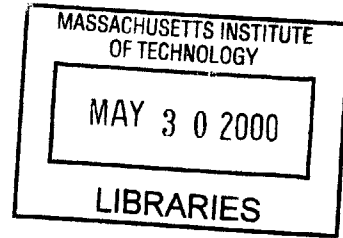


Controlling Wind Induced Motion in High-Rise Structures

By

Dereje Assefa

B.S. Civil Engineering
Virginia Polytechnic Institute and State University, 1995



ENG

SUBMITTED TO THE DEPARTMENT OF CIVIL AND ENVIRONMENTAL
ENGINEERING IN PARTIAL FULLFILLMENT OF THE REQUIREMENTS FOR
THE DEGREE OF

MASTER OF ENGINEERING
IN CIVIL AND ENVIRONMENTAL ENGINEERING

AT THE

MASSACHUSETTES INSTITUTE OF TECHNOLOGY

JUNE 2000

© 2000 Dereje Assefa. All rights reserved

The Author hereby grants MIT permission to reproduce
and to distribute publicly paper and electronic
copies of this thesis document in whole or in part

Signature of Author:

Department of Civil and Environmental Engineering
May 4, 2000

Certified By:

Jerome J. Connor
Professor of Civil and Environmental Engineering
Thesis Supervisor

Accepted By:.....

Daniele Veneziano
Chairman, Departmental Committee on Graduate Students

Controlling Wind Induced Motion in High-Rise Structures

By

Dereje Assefa

SUBMITTED TO THE DEPARTMENT OF CIVIL AND ENVIRONMENTAL
ENGINEERING IN PARTIAL FULLFILLMENT OF THE REQUIREMENTS FOR
THE DEGREE OF MASTER OF ENGINEERING
IN CIVIL AND ENVIRONMENTAL ENGINEERING

Abstract

Wind induced motion, which includes deflection, velocity and acceleration, is the governing condition for the lateral design of high-rise structures. Therefore, understanding the characteristics of wind and its application as a dynamic load is vital, and constitutes the major portion of the effort involved in the design of high rise structures for wind loading. The remaining effort concerns the conceptualization of a structural system that limits the motion induced by wind loading to recommended code values.

In this thesis, the characteristics of wind are discussed and the analysis in the frequency domain, of a two-degree of freedom system subjected to dynamic wind load is presented. The advantages of aerodynamically shaped buildings in reducing the applied wind load are identified. Lastly, the use of different types of manufactured dampers to significantly increase the damping ratio of a structure is described and illustrated.

Thesis Supervisor: Professor Jerome Connor

Title: Professor of Civil and Environmental Engineering

Acknowledgements

...to my parents....

I would like to thank my advisor, Professor Connor, for his guidance and support and without whom, I would not have been able to write this thesis.

I would like to thank my parents, Ato Assefa and W/o Alice, to whom I dedicate this thesis, for their unconditional love and support. I would like to thank my brothers Daniel and Alex, my twin sister Emebet, my cousin Dawit and his family and my uncle Tsegay, for their support.

I would like to thank my friends Grum and Brook for their support and special thanks to my girlfriend Chuchu for her understanding and support.

Table of Contents

Table of Figures	5
Introduction.....	6
1.0 Wind.....	8
1.1 Wind Characteristics	8
1.2 Dynamic Wind Load	11
1.2.1 Vortex Shedding.....	12
1.2.2 The Mathematics of Dynamic Wind Loading.....	14
1.2.3 Application of Dynamic wind load to Structures.....	21
1.2.4 Wind Tunnels	28
1.3 Wind Loading in Building Codes.....	35
1.3.1 Building Code of Canada	35
2.0 High Rise Structural Systems	39
2.1 Tubular Structures	39
2.2 Outrigger System.....	41
2.3 Braced Frame	42
3.0 Wind induced motion in High Rise Structures	44
3.1 Along wind response	45
3.2 Across wind response.....	45
3.3 Torsional Response	45
4.0 Controlling motion in High Rise Structures	46
4.1 Aerodynamics.....	46
4.1 Passive Control.....	47
Conclusion	55
Appendix I	56

Bibliography58

Table of Figures

Figure 1 Atmospheric Boundary Layer..... 9

Figure 2 – Mean and Turbulent Velocities in the Boundary Layer..... 10

Figure 3 Vortex Shedding 12

Figure 4 – Spectral Density Functions 18

Figure 5 – Aerodynamic Admittance Function..... 18

Figure 6 – Wind Tunnel 29

Figure 7 - Flexible Support Model..... 32

Figure 8 – Five-component force balance model..... 33

Figure 9 – Aeroelastic Model..... 34

Figure 10- Tubular Structures 39

Figure 11-Outrigger System..... 41

Figure 12-Brace Frame Structures 42

Figure 13 – Aerodynamically Shaped Buildings 46

Figure 14- Possible design for a viscous damper 51

Figure 15 – Fluid Viscous Dampers..... 52

Figure 16 Exposure Factor 56

Figure 17 Background Turbulence Factor..... 56

Figure 18 Size Reduction Factor..... 57

Figure 19 Gust Energy Ratio..... 57

Introduction

Tall buildings are one of the marvels of the engineering world. Once completed, they give the parties involved including the Architects, Engineers, owners and occupants, unimaginable satisfaction. They are also a source of pride for the community in which they are constructed. The race to house the tallest building in the world is evident today as cities in the USA, Asia and Europe continue to build high rises, one a few feet taller than the other.

This interest in high-rise structures present structural engineers with complex and extremely exciting challenges to develop new structural systems that will allow a high rise to be built taller than the previous tallest high rise.

The most important and challenging aspect in the design of high-rise structures is the effect of wind. As the height increases, the structure becomes more flexible and thus more vulnerable to wind loading. The motion measures resulting from wind loading are the displacements, velocities and accelerations at different elevations. One requirement that high-rises need to adhere to is the limit on acceleration of about 0.02g when subjected to a wind load with a return period of ten years. Other effects resulting from the response of a building to a dynamic wind loading such as screeching sounds of partition walls are also of concern and require the selection of a structural design that will keep them within the allowable limits.

In this thesis, the effects of wind loading on high-rise structures are examined and different ways of controlling these effects are discussed. The presentation is divided into four chapters. In chapter one, the phenomena associated with wind are discussed in detail. This discussion is followed by a description on how these phenomena are converted into loadings with mathematical expressions and applied to structures. Wind tunnel technology, which today is the most reliable technology for determining wind loading, is

described. Chapter one concludes with a discussion on how the current building codes handle the effects of wind loading on structures.

In chapter two, various types of high-rise structural systems are described. The emphasis is placed on how these systems behave under lateral loading. This chapter is included because one needs to understand the behavior of different structural systems before one can appreciate the rewards and methods of controlling wind induced motion in high rise structures. In chapter three, the response of buildings to dynamic loading is discussed. Different passive control strategies for controlling wind-induced motion are presented in chapter 4. Viscous dampers and equivalent viscous damping for visco-elastic, coulomb and hysteretic dampers are described. Chapter four ends with a discussion of the approach for distributing damping to obtain the optimal response with respect to the motion performance objectives.

1.0 Wind

1.1 *Wind Characteristics*

Wind or motion of air with respect to the surface of the earth, is fundamentally caused by variable solar heating of the earth's atmosphere. It is initiated by the difference of pressure between two points of equal elevation. More information on this topic is contained in chapter one of [1]. As the air moves with respect to the earth, the friction due to contact with the earth's surface exerts a drag force on the moving air. The effect of this force upon the flow decreases as the height above the ground increases and become negligible above a height δ known as the height of the *boundary layer*. It is the wind regime within the boundary layer of the earth's atmosphere that is of interest to the designer of civil engineering structures. The height δ of the boundary layer ranges from a few hundred meters to a few kilometers depending on roughness of the terrain.

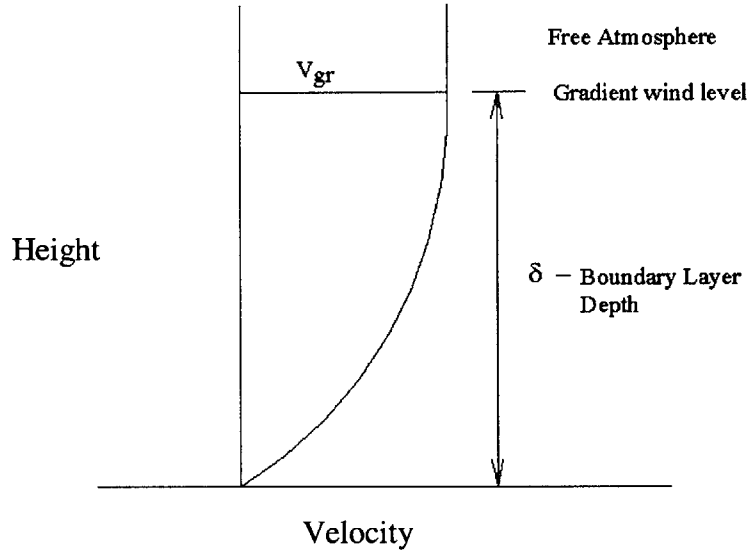


Figure 1 Atmospheric Boundary Layer

The drag force causes the velocity of the wind to be essentially zero at the ground surface and increase gradually with increasing height to a velocity V_{gr} , known as the gradient wind velocity. The profile of the wind velocity within the boundary layer, shown in Figure 1, is referred as the mean wind speed and is described by a logarithmic law that is defined later.

The smooth profile that represents the mean wind velocity in Figure 1 does not entirely describe the characteristics of the wind within the boundary layer. In addition to the mean velocity, there is a fluctuating wind speed component. The fluctuation varies randomly with time but is considered stationary, and fluctuates about the mean wind profile. Figure 2 is a better representation of the characteristics of wind within a boundary layer. The fluctuations occur mainly because of roughness of terrain.

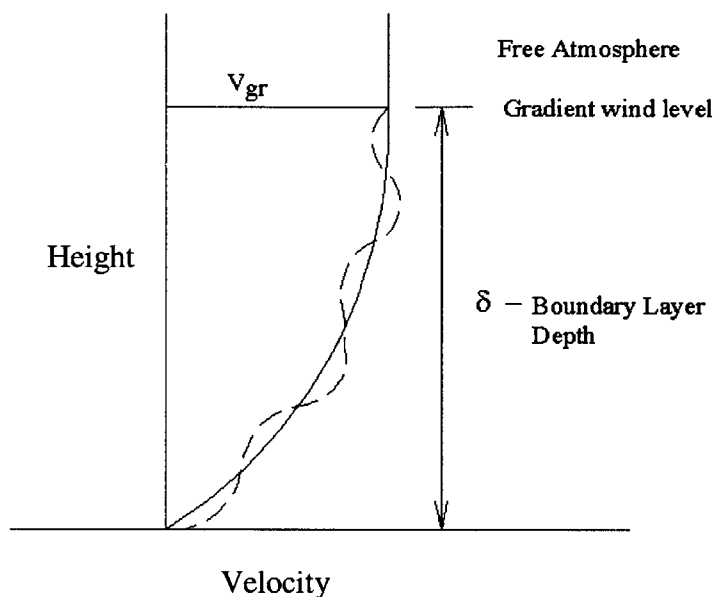


Figure 2 – Mean and Turbulent Velocities in the Boundary Layer

In low-rise structures the effects of the fluctuating wind speed are minimal and thus are less of a concern in design. However, in high-rise structures, which are generally more flexible, the effects of fluctuating wind speed cannot be ignored as they may occur in frequencies that coincide with one or more of the natural frequencies of the structure. This coincidence can lead to a dynamically amplified response of the structure, which may cause discomfort to building occupants or even lead to catastrophic failures. The famous Tacoma Narrows Bridge, although not a high rise, collapsed because of the effects of dynamic wind loading.

Determining the loading on high-rise structures as a result of the fluctuating wind speed is very complex. Yet in most cases, it is the primary loading that governs the design. The aerodynamic information needed to estimate the overall as well as the local wind effects cannot be determined from theory and must be obtained from experiments conducted in wind tunnel tests where all the effects that may cause these velocity fluctuations are modeled. However for a number of common situations, empirical formulas that provide

the aerodynamic information are available and procedures for estimating the structural response, which incorporate that information, may be employed.

In the sections that follow, the characteristics of dynamic wind loading are examined. The mathematics of dynamic wind loading is briefly described and an example that illustrates the application of these loads on structures is included. Lastly, how current building codes in Canada handle the effects of dynamic wind loads is then discussed

1.2 Dynamic Wind Load

As mentioned earlier, the wind velocity is defined by two quantities, a mean velocity $U(z)$ and a turbulent component $u(x,y,z,t)$. The loads from the mean wind speed may be treated as a static pressure that varies with height in the same manner as the mean wind velocity. The load is a function of the mean wind velocity, the density of air and the shape of the structure. The dependence on the shape of the structure is accounted for by a pressure coefficient C_p , which is obtained from wind tunnel tests.

The load from the turbulent component of the wind cannot be defined by a single formula. Since it varies with time and space, a statistical approach is used to characterize the effects of turbulent wind. The statistical approach, which is described in detail in the section under “the mathematics of wind”, provides a reasonable prediction of the wind loads. However, wind tunnel tests have proven to be the most reliable way of determining the load from the turbulent component of the wind.

1.2.1 Vortex Shedding

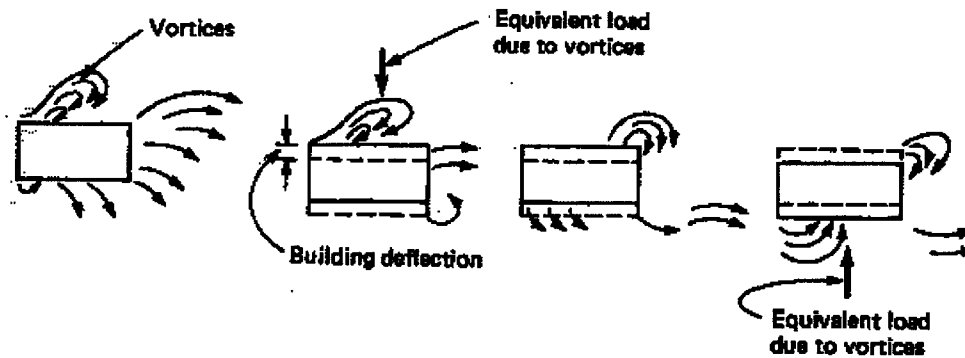


Figure 3 Vortex Shedding

The characteristics of wind that have been discussed thus far are the characteristics before the wind comes in contact with a structure. The effects of wind after it encounters a structure, is very important and needs to be included in the list of wind induced forces. As wind in a free stream encounters a structure, it is deflected around the structure and accelerated such that the velocity passing the upwind corners is greater than the velocity approaching the structure. The high-velocity fluid cannot negotiate the sharp corners and thus separates from the structure leaving a region of high negative pressure. The separated flow forms a shear layer on each side and subsequent interaction between the layers results in their rolling up into discrete vortices that are shed alternately. The difference in pressure between one side of the building and the other created as a result of the flow separation introduces forces on the building that are perpendicular to the direction of flow (see Figure 3). The alternating nature of the vortices makes these forces time dependant. The frequency at which these vortices are shed and thus the frequency of the load, is defined in terms of the Strouhal number:

$$N_s = \frac{U}{D} S$$

where

N_s = Frequency of full cycles of vortex shedding

D = Characteristic dimension of the body normal to the mean flow velocity

U = The mean velocity

S = The Strouhal Number

The Strouhal number depends on the shape of the structure. The Strouhal number for different shapes are given in [1].

The Strouhal number predicts the frequency of across wind load for a given mean wind velocity and a standard building shape. However, it does not give the magnitude of the force. Furthermore, the Strouhal number is only limited to certain known shapes and therefore the formulation is not applicable for irregular shapes. Once again one has to resort to the wind tunnel tests to assess the effects of vortex shedding on an irregular structure.

1.2.2 The Mathematics of Dynamic Wind Loading

The following notation is introduced

$A(n)$	=	Aerodynamic Admittance function
F_d	=	Drag Force – Force in the along wind direction
F_L	=	Lift Force – Force in the across wind direction
C_d	=	Drag Coefficient
C_L	=	Lift Coefficient
ρ	=	Mass Density of Air
$U(z)$	=	Mean Wind Speed
A_d	=	Applicable area in the along wind direction
A_c	=	Applicable area in the across wind direction
$S_u(n)$	=	Spectral Density Function for fluctuating velocity
$S_{f_j^c}^c(n)$	=	Cross-Spectral Density Function
κ	=	Peak factor
ω_i	=	natural frequency of structure

Wind loading can be mathematically dealt with in either the time domain or the frequency domain. In this thesis, the frequency domain analysis of wind loading is discussed.

The mathematics involved in calculating wind forces on rigid structures involves the evaluation of the mean wind speed $U(z)$ at a height z and the description of the statistical characteristics of fluctuating wind velocity $u(t)$ at that same height z above the ground surface. In this section, the mathematics of both mean and turbulent wind is described.

Mean Wind Speed.

The mean wind speed is shown in Figure 2 as the solid line. It varies from zero at the ground surface to a gradient velocity a distance δ above the ground surface. For the purposes of design however, the mean wind velocity is taken to be constant for the first 10 meters. The mean wind speed profile is described by a logarithmic law that gives the mean speed $U(z)$ at a height z above the ground as;

$$U(z) = 2.5u_* \ln\left(\frac{z}{z_0}\right)$$

where

$$u_* = \frac{U(10)}{2.5 \ln(10/z_0)}$$

or

$$u_* = U(10)\sqrt{k}$$

z_0 = Roughness length above ground surface. (See Table 1.1)

k = Surface drag coefficient

Type of Terrain	z_0	k
Sand	0.0001-0.001	1.2-1.9
Sea Surface	0.005	0.7-2.6
Low Grass	0.01-0.04	3.4-5.2
High Grass	0.04-0.10	5.2-7.6
Pine Forest	0.9-1.00	28.0-30.0
Suburban areas	0.20-0.40	10.50-15.40
Center of Cities	0.35-0.45	14.20-16.60
Centers of Large Cities	0.60-0.80	20.20-25.10

Table 1.1 Roughness lengths and surface drag coefficients for various types of terrains

The drag force and the lift force due to mean wind velocity are given by;

$$F_d = \frac{1}{2} \rho C_d A_d U(z)^2$$

$$F_L = \frac{1}{2} \rho C_L A_L U(z)^2$$

Statistical Properties of the fluctuating velocity component of wind

Velocity measurements have shown that the velocity of the fluctuating wind can be considered as a stationary random process. This means that the velocity fluctuates with a mean of zero and does so about the mean wind velocity. Because of this property the fluctuating component of the wind can be quantified by statistical functions. For the purposes of dynamic analysis, the most important of these functions are;

- The variance σ^2 and standard deviation σ
- The spectral density function or power spectrum $S_u(n)$
- Aerodynamic Admittance Factor
- The cross-spectral density and the Coherence function
- The Modal Forces Spectra
- The Response Spectra
- The peak factor κ

A detailed derivation of these functions is contained in [1] and [9].

The variance σ^2 and standard deviation σ

The variance of the fluctuating or gust velocity component is defined as;

$$\sigma^2(u_x) = \frac{1}{T} \int_0^T u_x^2(t) dt$$

In multi-degree of freedom systems the variance of the principal coordinates is given by;

$$\sigma^2_{q_i} = \int_0^{\infty} S_{q_i} d\omega$$

For Civil Structures, which are considered lightly damped, the variance can be given by;

$$\sigma^2_{q_i} = S_{q_i} \Delta\omega = S_{q_i} \frac{1}{2} \xi_i \omega_i$$

Spectral Density Functions

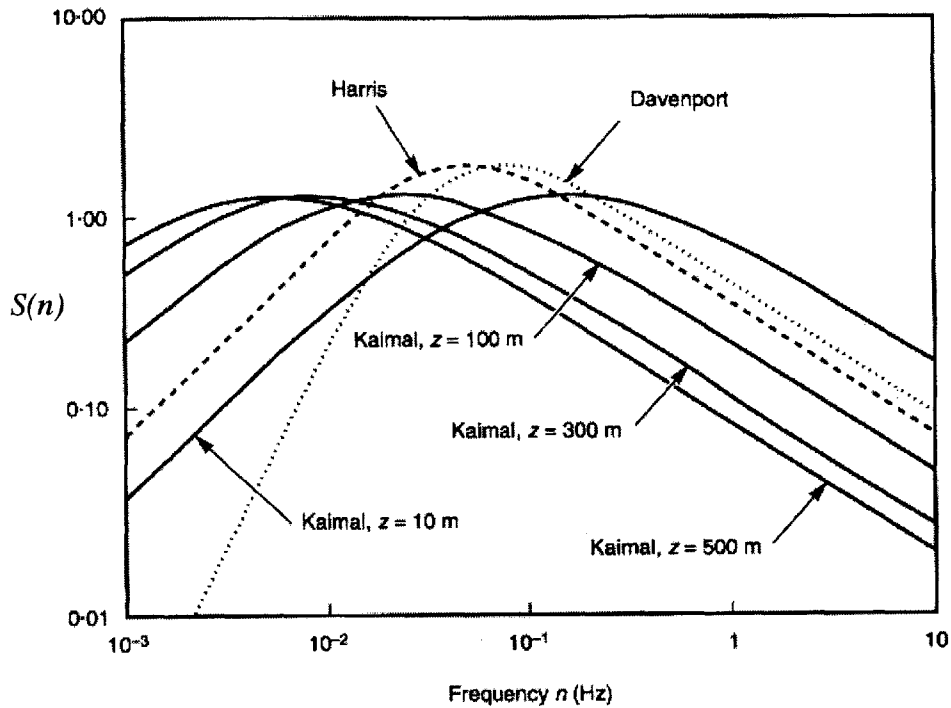
The Spectral Density function also referred to as the power spectra describe the random nature of the wind. It provides a measure of the energy distribution of the harmonic velocity components, and forms the basis for dynamic response analysis of linear structures in the frequency domain. Different researchers have suggested different formulation for the spectral density function. The equations are presented below and the corresponding graphs are shown in Figure 4.

$$S_u(n) = \frac{4u_*^2 f^2}{n(1+f^2)^{4/3}} \quad ; \quad f = \frac{1200n}{U(10)} \quad \text{Davenport}$$

$$S_u(n) = \frac{0.115\sigma^2(z)T_u(z)}{\{0.0141 + n^2 T_u^2(z)\}^{5/16}} \quad \text{Deaves and Harris}$$

where $T_u = \frac{L_u^z}{U(z)}$; $L_u^z = 0.6z^{0.5}$ = integral length scale

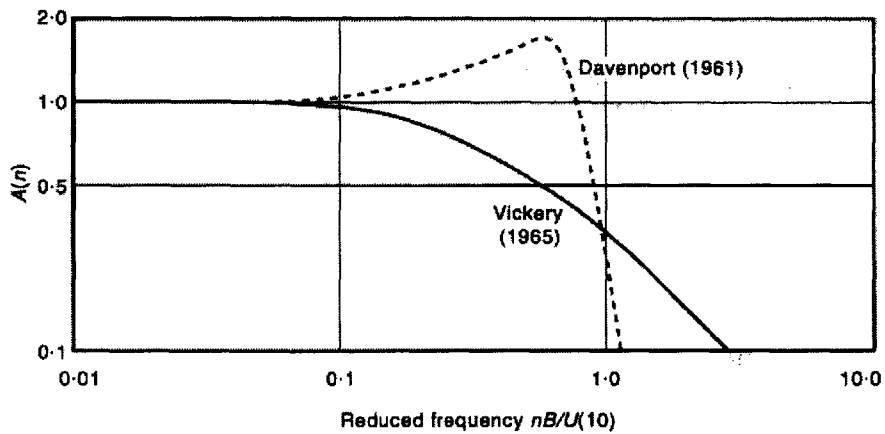
$$S_u(n) = \frac{200u_* f(z,n)}{n[1+50f(z,n)]^{5/3}} \quad ; \quad f = \frac{zn}{U(z)} \quad \text{Kaimal}$$



Comparison of spectral density functions for $U(10) = 30 \text{ m/s}$ and $z_0 = 0.08 \text{ m}$

Figure 4 – Spectral Density Functions

Aerodynamic Admittance Function $A(n)$:



Variation of the aerodynamic admittance factor $A(n)$ with the reduced frequency $nB/U(10)$: the value B is a structural reference dimension, n corresponds to a structural mode frequency, and $U(10)$ is the reference wind velocity

Figure 5 – Aerodynamic Admittance Function

The Cross-spectral density function and coherence functions for load resulting from longitudinal velocity fluctuation.

The Cross-spectral density function, which is approximately equal to the co-spectrum, and coherence functions for the longitudinal velocity fluctuations are given by;

$$S^c_{f_j f_k}(n) = [\sqrt{[S_{f_j}(n) * S_{f_k}(n)]}] * e^{-\phi}$$

where

$$S_{f_j} = 4 \frac{F^2(z_j)}{U^2(z_j)} A(n) S_{u_j}(n)$$

$$S_{f_k} = 4 \frac{F^2(z_k)}{U^2(z_k)} A(n) S_{u_k}(n)$$

$e^{-\phi}$ is the square root of the coherence function $coh^2_{u_j u_k}(n)$

where

$$\phi = \frac{2n \sqrt{C_x^2 (x_j - x_k)^2 + C_y^2 (y_j - y_k)^2 + C_z^2 (z_j - z_k)^2}}{U(z_j) + U(z_k)}$$

and $C_z = 8$; $C_y = 16$

The Cross-spectral density function gives a measure of the degree to which two histories $u(t)$ and $v(t)$, recorded at a station j and k are correlated in the frequency domain.

The modal force Spectrum

The modal force spectrum is given by

$$S_{f_{q_i}} = Z_i^T S_{jk}^c Z_i$$

where Z_i is the modal vector normalized with respect to the modal mass.

The Response Spectrum for the i^{th} principal coordinates q_i

$$S_{q_i}(\omega_i) = \frac{M(\omega_i) S_{f_{q_i}}}{\omega_i^4}$$

where $M(\omega_i)$ is referred to as the Mechanical Admittance Factor is the square of the transfer function, which is referred to H_1 or H_2 in [8] and varies depending on what type of response one wants to obtain. For example the Mechanical Admittance Factor if one is interested in displacement is.

$$M(\omega_i) = \frac{1}{4\xi_i^2}$$

The peak factor κ for $u(t)$

The magnitude of the amplitude of the maximum fluctuation that may occur within a given time interval T is given by;

$$q_{\max} = \kappa \sigma_{q_i}$$

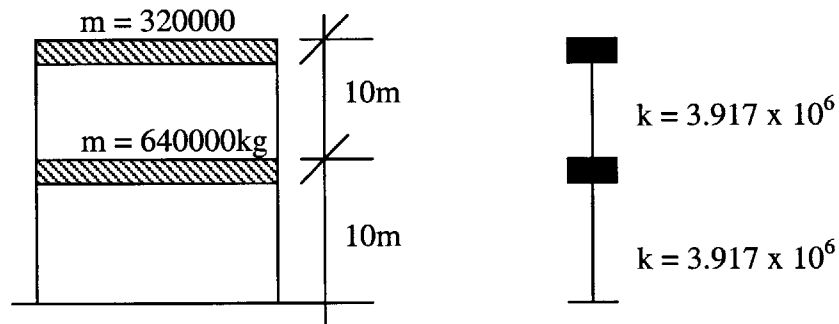
where

$$\kappa = \sqrt{2 \ln(2\pi w_n T)} + 0.577 \sqrt{2 \ln(2\pi w_n T)}$$

$$T = 3600\text{s}$$

1.2.3 Application of Dynamic wind load to Structures

In the previous section, the formulas required to define wind as a dynamic loading were presented. In this section, these formulas are applied to a shear building idealized as a 2-degree of freedom structure with plan dimensions of 10m by 10m and the following properties.



Suppose the maximum displacement at 20meters above the ground surface is desired when the system is subjected to a dynamic wind load with the following properties:

- Roughness length $z_0 = 1.0$ (Pine forest)
- Mean Wind Speed at 10m $U(10) = 30$ m/s
- Power spectrum suggested by Davenport
- $C_d = 2.0$

The calculation of the desired displacement involves 14 steps and is presented next.

□ **Step 1 – Evaluate natural frequencies and modal properties**

$$\underline{M} = \begin{bmatrix} 320000 & 0 \\ 0 & 640000 \end{bmatrix} \quad ; \quad \underline{K} = \begin{bmatrix} 7.834 * 10^6 & -3.917 * 10^6 \\ -3.917 * 10^6 & 3.917 * 10^6 \end{bmatrix}$$

Solving the eigenvalue problem, the natural frequencies ω of mode 1 and mode 2 and the corresponding mode shape vectors are given by;

$$\underline{\omega} = \begin{bmatrix} 27.917 \\ 2.683 \end{bmatrix} ; \quad \underline{\Phi} = \begin{bmatrix} 0.963 & -0.49 \\ 0.27 & -0.872 \end{bmatrix}$$

The Modal Mass is given by;

$$\begin{aligned} \phi_1^T \underline{M} \phi_1 &= \tilde{m}_1 &= 5.654 * 10^5 \\ \phi_2^T \underline{M} \phi_2 &= \tilde{m}_2 &= 3.434 * 10^5 \end{aligned}$$

The mode shapes normalize the with respect to the modal mass is given by;

$$\underline{Z} = \frac{\underline{\Phi}_{ij}}{\tilde{m}_i} = \begin{bmatrix} 2.808 * 10^{-6} & -8.773 * 10^{-7} \\ -7.872 * 10^{-7} & -1.542 * 10^{-6} \end{bmatrix}$$

□ **Step 2 – Evaluate the mean wind speed at elevation 20m and 10m**

$$\begin{aligned} u_* &= \frac{30}{2.5 \ln(10)} &= 5.212 \text{m/s} \\ U(20) &= 2.5 * 5.212 * \ln\left(\frac{20}{1}\right) &= 39.03 \text{m/s} \end{aligned}$$

$$U(10) = 2.5 * 5.212 * \ln\left(\frac{10}{1}\right) = 30\text{m/s}$$

- **Step 3 – Evaluate F_d , force due to mean wind velocity**

$$F_d(10) = \frac{1}{2} * 1.226 * 2.0 * 10 * 10 * 30^2 = 110340\text{N}$$

$$F_d(20) = \frac{1}{2} * 1.226 * 2.0 * 10 * 10 * 39.03^2 = 186800\text{N}$$

$$\underline{F_d} = \begin{bmatrix} 186800 \\ 110340 \end{bmatrix} \text{N}$$

- **Step 4 – Calculate the Static Response**

$$\underline{X_s} = K^{-1} F_d$$

$$\underline{X_s} = \begin{bmatrix} 0.076 \\ 0.124 \end{bmatrix}$$

- **Step 5 – Calculate the values of the velocity spectrum**

Using power spectrum proposed by Davenport for $n = \frac{\omega}{2\pi}$

$$S_u(n) = \frac{4u_*^2 f^2}{n(1+f^2)^{4/3}} \quad ; \quad f = \frac{1200n}{U(10)}$$

$$f(2.683) = \frac{1200 * 2.683}{30 * 2\pi} = 17.081$$

$$S_u(2.683) = \frac{4 * 5.212^2 * 17.081^2 * 2\pi}{2.683(1 + 17.081^2)^{4/3}} = 50.79$$

$$f(27.917) = \frac{1200 * 27.917}{30 * 2\pi} = 177.73$$

$$S_u(27.917) = \frac{4 * 5.212^2 * 177.73^2 * 2\pi}{27.917(1 + 177.73^2)^{4/3}} = 0.47$$

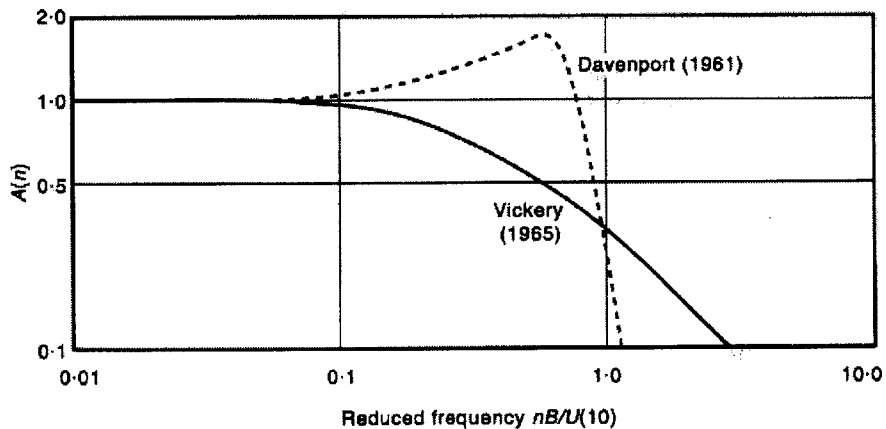
□ **Step 6 – Calculate the Aerodynamic Admittance Function**

First mode

$$\frac{nB}{U(10)} = \frac{2.683 * 10}{30 * 2\pi} = 0.142 ; \text{ From Graph } A(n) = 1.2$$

Second mode

$$\frac{nB}{U(10)} = \frac{27.917 * 10}{30 * 2\pi} = 1.481 ; \text{ From Graph } A(n) = 0.1$$



Variation of the aerodynamic admittance factor $A(n)$ with the reduced frequency $nB/U(10)$: the value B is a structural reference dimension, n corresponds to a structural mode frequency, and $U(10)$ is the reference wind velocity

□ **Step 7 – Calculate the values of the force spectrum**

$$S_{fd} = 4 \frac{F^2(z)}{U^2(z)} A(n) S_u(n)$$

$$S_{f_{11}} = 3.293 * 10^9$$

$$S_{f_{21}} = 4.309 * 10^6$$

$$S_{f_{12}} = 2.546 * 10^6$$

$$S_{f_{22}} = 5.573 * 10^9$$

□ **Step 8 – Calculate the Square root of the coherence function**

$$e^{-\phi}$$

$$\phi = \frac{\omega_i \sqrt{C_z^2 (z_j - z_k)^2}}{\pi (U(z_j) + U(z_k))}$$

$$\phi_1 = 0.99$$

$$e^{-\phi_1} = 0.372$$

$$\phi_2 = 0.99$$

$$e^{-\phi_2} = 0.372$$

□ **Step 9 – Cross-spectra density functions**

For first mode;

$$S_{11}^c(n) = \left[\sqrt{[S_{f_1}(n) * S_{f_1}(n)]} * e^{-0} \right] = 3.293 * 10^9$$

$$S_{12}^c(n) = S_{21}^c = \left[\sqrt{[S_{f_1}(n) * S_{f_2}(n)]} * e^{-\phi} \right] = 4.427 * 10^9$$

$$S_{22}^c(n) = \left[\sqrt{[S_{f_2}(n) * S_{f_2}(n)]} * e^{-0} \right] = 4.309 * 10^9$$

$$\underline{S_1^c} = \begin{bmatrix} 3.293 * 10^9 & 4.427 * 10^7 \\ 4.427 * 10^7 & 4.309 * 10^6 \end{bmatrix}$$

For Second mode;

$$S_{11}^c(n) = \left[\sqrt{[S_{f_1}(n) * S_{f_1}(n)]} * e^{-0} \right] = 3.293 * 10^9$$

$$S_{12}^c(n) = S_{21}^c = \left[\sqrt{[S_{f_1}(n) * S_{f_2}(n)]} * e^{-\phi} \right] = 4.013 * 10^3$$

$$S_{22}^c(n) = \left[\sqrt{[S_{f_2}(n) * S_{f_2}(n)]} * e^{-0} \right] = 4.309 * 10^6$$

$$\underline{S_2^c} = \begin{bmatrix} 3.293 * 10^9 & 4.013 * 10^7 \\ 4.013 * 10^7 & 4.309 * 10^6 \end{bmatrix}$$

- **Step 10 – Calculate the force spectrum for each mode**

$$S_{f_{q_i}} = Z_i^T \underline{S_i^c} Z_i$$

$$S_{f_{q_1}} = 2.664 * 10^{-3}$$

$$S_{f_{q_2}} = 0.026$$

- **Step 10 – Calculate the Response Spectrum for the principal coordinates**

$$S_{q_i}(\omega_i) = \frac{M(\omega_i) S_{f_{q_i}}}{\omega_i^4}$$

$$M(\omega_i) = \frac{1}{4\xi_i^2}$$

$$S_{q_1} = 5.141 * 10^{-3}$$

$$S_{q_2} = 0.05$$

- **Step 11 – Calculate the Variance**

$$\sigma_{q_i} = \sqrt{\frac{S_{q_i} \xi_i \omega_i}{2}}$$

$$\sigma_{q_1} = 0.026$$

$$\sigma_{q_2} = 0.085$$

- **Step 12 – Calculate Peak Factor**

$$\kappa = \sqrt{2 \ln(2\pi w_i T)} + 0.577 \sqrt{2 \ln(2\pi w_i T)}$$

$$\kappa_1 = 6.364$$

$$\kappa_2 = 7.225$$

□ **Step 13 – Calculate q**

$$q_i = \sigma_i \kappa$$

$$q_1 = 0.167$$

$$q_2 = 0.613$$

□ **Step 14 – Calculate displacement**

$$\underline{X} = \underline{Z}q$$

$$\begin{bmatrix} x_1 \\ x_2 \end{bmatrix} = \begin{bmatrix} z_{11} & z_{12} \\ z_{21} & z_{22} \end{bmatrix} \begin{bmatrix} q_1 \\ q_2 \end{bmatrix} = \begin{bmatrix} -0.139 \\ -0.58 \end{bmatrix}$$

1.2.4 Wind Tunnels

As was suggested in previous sections, wind loading varies with time and space and in a random way. These loads also vary with the shape of the structure. For that reason formulas presented in the earlier section is at best an approximation of the load. The most reliable way of determining the wind load on a structure is to carry out wind tunnel tests. In the following section, the process involved and the results obtained from a wind tunnel test are discussed.



Figure 6 – Wind Tunnel

In wind tunnels designed for civil structures, a scaled down version of the turbulent boundary layer is recreated and applied to a scaled down model of the structure for which wind load information is to be obtained. The area surrounding the structure is also modeled so that the effects of any surrounding structure on the turbulent wind profile are accounted for (see Figure 6). The devices used to recreate the turbulent boundary layer are described in detail in [4]. The main objective of a wind tunnel test on high-rise structures is to obtain the following;

- ❑ Wind Loads on the Cladding and Glass
- ❑ Fluctuating Loads for determining the dynamic response
- ❑ Building Motion - Wind load interaction

Although not common, model testing is done on building configurations to determine the most favorable shape of the building for wind. As will be shown in chapter four, the shape of a building can influence the effects of wind on that structure.

There are three different types building models used in wind tunnel tests: *the rigid pressure model*; *the rigid high-frequency force balance model*; and the *aeroelastic model*. One or all three models can be used to determine the design information listed above.

However, the cost and the time it takes to construct all three models become prohibitive for all but a few high budget structures. Usually, two of the three models namely, the rigid pressure model, and the rigid high-frequency force balance model, are used. The latter was created by wind tunnel engineers as a substitute to the more expensive but highly accurate aeroelastic model. The different models have different characteristics and are discussed below ~~and are discussed below~~.

The Rigid Pressure Model

The Rigid Pressure model is primarily used to study the local pressure fluctuations on a building for the purposes of designing the cladding. Cladding pressure study is of great concern because of the large number of inadequately performing or failed curtain wall systems in the US. Although some more advanced building codes have attempted to establish design loads with due considerations to shape factors, turbulence and dynamic characteristics of buildings, it has become industry practice to resort to wind tunnel tests because it generally felt by owners and developers that the confidence in wind loads obtained from wind tunnel tests far out weigh the costs. In fact most curtain wall suppliers for high-rise building hesitate to undertake a job if the cladding pressure studies are not available.

In rigid pressure model, significant effort is put into modeling the features of the building that affect the wind flow as it comes in contact with the building. These features include the profile of the building, protruding mullions and overhangs. Because the model is rigid, no attempt is made to simulate the dynamic responses of the building.

The model is instrumented with a large number of pressure taps. Flexible transparent vinyl or polyethylene tubing is used as pressure tapping and is usually distributed around the face of the model with more concentrations in regions of high-pressure gradient such as building corners. The pressure tapings are connected to miniature electronic pressure transducers that allow the measurement of pressure fluctuations. The model of the building along with the model of the surrounding area is placed on a rotating base so that

wind action is modeled from different directions. Usually wind directions are modeled about 10 degrees apart. The data is then converted into pressure coefficients. From the data, full scale peak exterior pressures and suctions for the selected return periods at each tap locations are derived by combining the wind tunnel data with a statistical model of windstorms expected at the building site. This data is condensed into recommended cladding design loads and presented to the engineer in the form of block diagrams. Examples of such diagrams are shown in [4].

High-Frequency Force balance Model

In a tall building the effect of wind load can be looked upon as created from two distinctly different contributions.

The mean wind load

Fluctuating load resulting from Turbulence

The Rigid pressure model described above offers a convenient method of obtaining the local wind pressures on the building faces. However, these pressures do not include the influence of gust and there fore need to be multiplied by a conservative gust factor if one wants to use them to design the lateral force resisting system of a building.

An alternative method is to eliminate the guesswork out of the gust factor calculations and determine them experimentally. To do that, one needs create a model that will allow you to actually measure these dynamic effects. The high-frequency force balance model is such a model. There are two types of force balance models, *flexible support model* and *five Component Force Balance model*.

Flexible support model

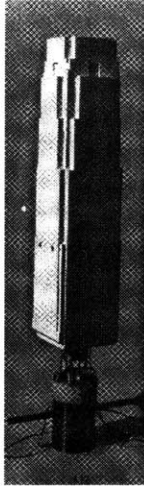


Figure 7 - Flexible Support Model

In the flexible support model (Figure 7), the outer shell of the model representing the architectural shape of the building is connected to a flexible metal cantilever bar. Accelerometers and strain gauges are fitted into the model. Instead of measuring the dynamic forces on the entire height of the building, the dynamic bending moments are measured at the base of the building. Power spectral density functions are computed for these moments with appropriate corrections to remove the effects of modal resonance. The inertial forces at each floor are computed from the measured accelerations and from the knowledge of the building weight at that level. This method is applicable to buildings where the building motion does not itself affect the aerodynamic forces and where torsional effects are not of concern.

Five Component Force Balance model

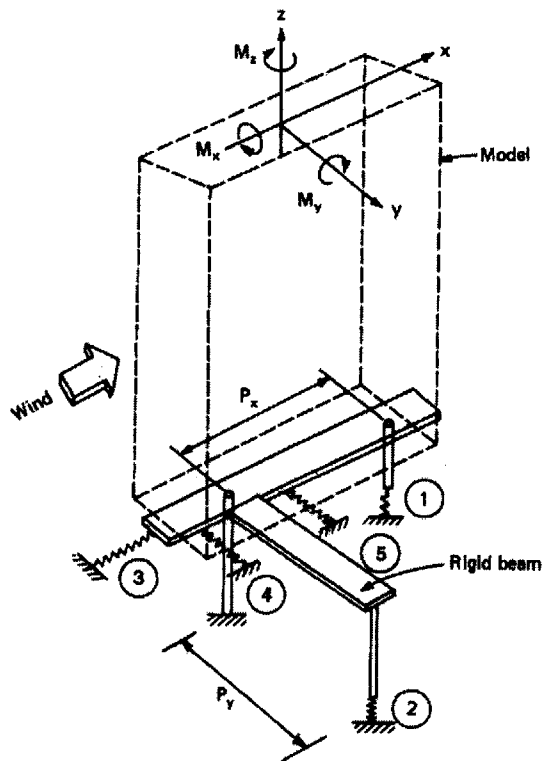


Figure 8 – Five-component force balance model

The five-component force balance model (Figure 8), involves a rigid model of the building made out of light material such as foam mounted on a five-component high-sensitive force balance. It is used to measure bending moments and shear forces in two orthogonal directions and torsion about the vertical axis.

In both methods, the resulting fluctuating loads on the model as a whole are determined, and by making certain simplifying assumptions, the information that is of interest to the structural engineer including the floor lateral loads and acceleration at the top of the building is calculated.

Aeroelastic Model

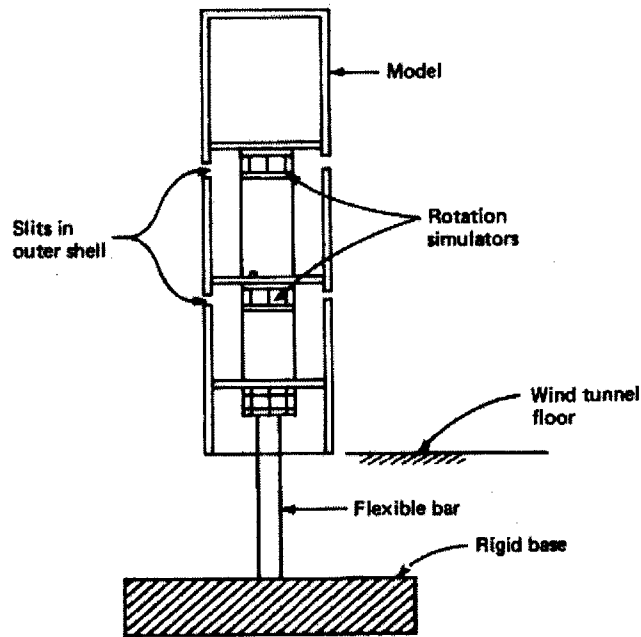


Figure 9 – Aeroelastic Model

Although good estimate of the of the mean wind loading can be obtained from the rigid pressure model and a somewhat accurate estimate of the dynamic loading from the frequency balance model, the best results from the dynamic loading effects of wind is obtained from an Aeroelastic Model of the building. The fluctuating aerodynamic loads can be measured from a variety of models ranging from very simple rigid models mounted on flexible supports to models exhibiting the multimode vibration characteristics of tall building. The elastic model is the most expensive of the three in terms of money and the amount of time it takes to build, but it is the only model that can provide a measurement of the load resulting from building wind interaction.

1.3 Wind Loading in Building Codes

1.3.1 Building Code of Canada

The National Building Code of Canada (NBC) has a somewhat simplified way of describing dynamic wind load and the application of dynamic wind loading to structures. It describes two approaches, the “simple procedure” which is appropriate for use in low and medium rise structures, and the “detailed procedure” which is primarily intended for determining the overall wind loading and amplified resonant response of tall buildings and slender structures. This section discusses the latter.

The detailed procedure consists of a series of calculations involving (a) the intensity of wind turbulence for the site as a function of height and the surface roughness of the surrounding terrain and (b) properties of the building such as height, width, natural frequency of vibration and damping. The end product of the calculation is the gust effect factor, C_g , which is multiplied by the reference wind pressure, q , the exposure factor, C_e , and the pressure coefficient, C_p , to give the static design pressure which is expected to produce the same peak load effect as the dynamic resonant response to the actual turbulent wind.

The Gust effect factor, C_g

The Gust effect factor is defined as the ratio of the maximum effect of the loading to the mean effect of the loading. A general expression for the maximum or peak loading effect, denoted W_p , is

$$W_p = \mu + g_p \sigma$$

where ;

μ = The mean loading effect

σ = The “root mean square” loading effect

g_p = A statistical peak factor for the loading effect

Then, the gust effect factor equal to the ratio of the peak loading to the mean loading, can be written as;

$$C_g = 1 + g_p \left(\frac{\sigma}{\mu} \right)$$

The value $\frac{\sigma}{\mu}$ can be expressed as;

$$\frac{\sigma}{\mu} = \sqrt{\frac{K}{C_{eH}} \left(B + \frac{sF}{\xi} \right)}$$

where K

K = a factor related to the surface roughness coefficient of the terrain

= 0.08 for Exposure A,

= 0.10 for exposure B,

= 0.14 for exposure C,

Exposure A - Reference exposure - Open level terrain with only scattered buildings or other obstructions.

Exposure B - Suburban and urban areas or wooded terrain.

Exposure C - Centers of Large Cities with concentration of Tall Buildings.

C_{eH}^* = exposure factor at the top of the building, H, evaluated according to Figure 16 in Appendix I.

B = Background Turbulence factor obtained from Figure 17 in Appendix I, as a function of W/H

W = Width of windward face of the building

H = Height of windward face of building

s = Size reduction factor obtained from Figure 18 as a function of W/H and the reduced frequency $n_o H/U(H)$

n_o = natural frequency of vibration, Hz,

$U(H)$ = mean wind speed (m/s) at the top of the structure, H

$$U(H) = U(10)\sqrt{C_{eH}}$$

where $U(10)$ is the reference wind velocity

F = gust energy ratio at the natural frequency of the structure obtained from Figure 19 in Appendix I

ξ = damping ratio.

Reference Wind Pressure, (q)

The reference wind pressure is determined from the reference wind velocity $U(10)$ using the following equation;

$$q = CU(10)^2$$

where C is a factor that depends on the atmospheric pressure and the air temperature.

The atmospheric pressure is in turn influenced by the elevation above sea level. Values for C are given in [10].

The Exposure Factor is needed in three different capacities. The first one is in calculating the hourly mean speed at the top of the structure being designed. The second is in the when calculating the gust effect factor C_g . The third is when calculating the pressures for the windward and leeward faces of tall buildings.

The exposure factor is slightly modified for structures on a hill. The modification is given in [10].

The Pressure Coefficient Cp

Pressure coefficients are the non-dimensional ratios of wind-induced pressures on a building to the dynamic pressure (velocity pressure) of the wind speed at the reference height. Pressure on the surface of a structure varies considerably with the shape, wind direction and profile of the wind velocity. Pressure coefficients are usually determined from wind tunnel experiments.

Vortex Shedding

The dynamic effects of vortex shedding for a cylindrical structure can be approximated by a static force acting over the top one-third of the structure in the direction perpendicular to the wind. The equivalent static force per unit height is given by;

$$F_L = \frac{C_1}{\sqrt{\lambda} \sqrt{5 - C_2 \frac{\rho D^2}{M}}} q_H D$$

ξ = Damping Ratio

λ = Aspect Ratio

H = Height of Structure

q_H = Velocity Pressure Corresponding to $U(H) \approx 0.6U(H)$

M = Average mass per unit length

ρ = Density of Air

C1 = 3 for $\lambda > 16$
 $3(\lambda)^{0.5}$ for $\lambda < 16$

C2 = 0.6

2.0 High Rise Structural Systems

2.1 Tubular Structures

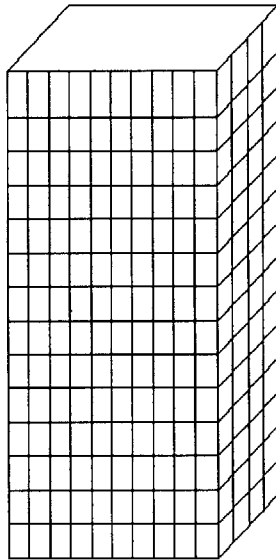


Figure 10- Tubular Structures

At present four of the world's largest buildings are tubular structures. They are the 110-story Sears Tower, the 100-story John Hancock Building and the 83-story Standard Oil Building, all in Chicago and the 110-story World trade center in New York.

The basic form that pioneered the use of tubular structures systems in high-rise buildings involve using closely spaced columns on the perimeter of the building. These columns, as part of a moment resisting frame, convert the high-rise structure to a pseudo tube thereby increasing the moment of inertia and the bending rigidity of the building. The pseudo tube, cantilevered from the ground acts as the main lateral force resisting system for the building. The frames parallel to the direction of the load act as the webs and the frames

perpendicular to the direction of the load act as the flanges. The structural optimization reduces to examining different column spacing and the member proportions.

Although the structure has a tube like form, its behavior is much more complex than the solid tube. Unlike the solid tube, it is subjected to shear lag effects that increase the axial stresses in the corner columns and reduces them in the interior columns. Shear lag effects are discussed more in [2]. In order to solve the shear lag problem, engineers have taken advantage of the need to place elevator shafts in the building. The elevator shafts, which are usually placed in the center of the building are made to act together with the outer tube in resisting lateral loads. This system, referred to as either *Tube in Tube* or *Hull-Core*, falls short of eradicating the shear lag problem because the large structural depth of the outer tube tend to dominate the force resisting capability of the building and thus little force is shared between the two tubes.

A variation to the tubular system that has been effective in eliminating the shear lag problem is the bundled tube structure. The bundled tube structure, which was successfully used in the Sears Tower in Chicago, provides interior webs that greatly reduce the effects of shear lag.

Another variation to the tubular structure that has proven to be effective in eliminating shear lag effects is the use of diagonal braces on the exterior of the building. This method was successfully used in the John Hancock building in Chicago. The presence of the diagonal braces also allows for larger column spacing, which opens the interior of the building to more sunlight

2.2 Outrigger System

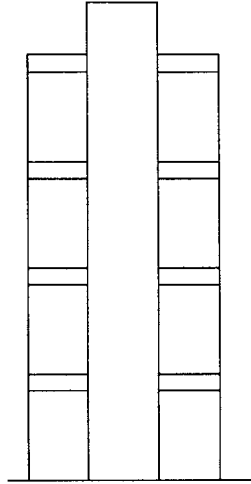


Figure 11-Outrigger System

This structural system consists of a central core, comprising of either shear walls or braced frames from which “outrigger trusses” are cantilevered. These outriggers are in turn connected to exterior column which , depending on the direction of the load, go in tension or compression to resist rotation of the outrigger truss and thus the core. This system in effect increases the structural depth of the building thereby decreasing the moment and deflection of the core.

Perimeter columns other than those connected directly to the end of the outriggers can also be made to participate in the outrigger action by joining all the perimeter columns by a “belt truss” or girder around the face of the building at the outrigger level.

An outrigger system can have just one outrigger at the top, which is referred to as the “Top Hat” or can have multiple outriggers throughout the height of the building. Having multiple outriggers has been shown to be beneficial and more effective in controlling motion, however, each additional outrigger performs less than the previous one. For that

reason, the optimum number of outriggers is between three or five for a typical high rise (50 to 70 stories).

While outriggers are effective in resisting flexural loads and controlling deflection, they are not as effective in resisting shear loads. The entire shear has to be resisted by the core.

2.3 Braced Frame

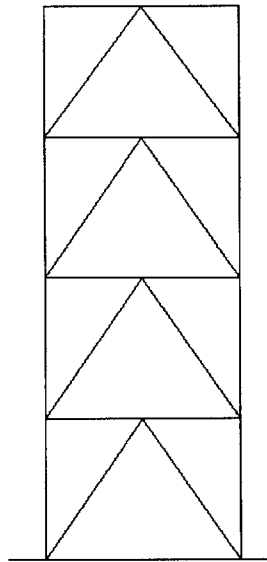


Figure 12-Brace Frame Structures

Bracing is a highly efficient and economical method of resisting horizontal forces in a frame structure. A braced bent consists of the usual column and girders, whose primary purpose is to support the gravity loads and diagonal bracing members that are connected so that the total set of members form a vertical cantilever truss while the column act as the chords.

The system is efficient because all the forces are resisted by the most efficient way, which is by axial action. Most of the world's earlier structures were designed using bracing, the most famous of which is New York's Empire State Building. Usually, these braces are installed between floors but recently, new forms of bracing have been used that span multiple stories.

Diagonal Bracing is inherently obstructive to the architectural plan and can cause problems in organizing internal space. The most efficient but also the most obstructive type of bracing is one that forms a fully triangulated vertical truss. These include single diagonals double diagonals and K-braces.

3.0 Wind induced motion in High Rise Structures

The elements of high-rise structures need to be designed to resist all the applied forces. In addition, serviceability requirements that come in the form of a limit on acceleration or limit on maximum deflection need to be satisfied. This design procedure follows the traditional method where the members are designed for strength and checked for serviceability.

Wind induced motion is a major concern in the design of today's high-rises. The introduction of high strength materials with no appreciable increase in stiffness properties is leading to more flexible structures whose design is governed by motion rather than strength. As a result the design process has been flipped where the lateral resisting members of a high-rise structure are designed to satisfy serviceability considerations and checked to comply with strength requirements. This method is referred to as motion-based design. The methods and design of different motion controlling devices are discussed in Chapter 4.

The major serviceability limits that need to be addressed in the design of high-rise structures are that of maximum deflection and acceleration. The deflection of a building relative to the surrounding objects creates an unpleasant feeling to the occupants of that building. For that reason the wind induced maximum deflection of a building, which usually occurs at the top, is limited to $H/500$, where H is the height of the building. This limit usually is required to be satisfied for wind loads that come once every 10years.

The acceleration of the building also creates a discomfort to occupants of that building. A number of studies that have been conducted on existing high-rise buildings indicate that occupants are perceptive to the motion of a building if the acceleration reaches 2 percent of gravity ($0.02g$). As a result the limit on the wind-induced acceleration of a building, which usually happens at the top of the building, is limited to $0.02g$ under a 10year wind.

The response of buildings subjected to wind loads, be it acceleration, deflection or velocity, come in different forms, three of which are the along wind response, the across wind response and the torsional response. These three are dominant responses and are discussed in the sections below.

3.1 Along wind response

The along wind response of a building due to wind loading is its response in the direction of the wind. This response is due to the action of the mean wind speed and the fluctuating wind speed. The along wind response is dynamic and depends primarily on critical damping ratio, the natural frequency of the structure and the frequency of the forcing function, all in the direction of the wind.

3.2 Across wind response

The across wind response is caused by the vortex shedding phenomena. Figure 1.2 shows the motion of a structure due to alternating vortices. The response is dynamic, and as the along wind response, depends on the frequency of the forcing function, , the natural frequency of the structure and the critical damping ratio, all in the direction perpendicular to that of the wind.

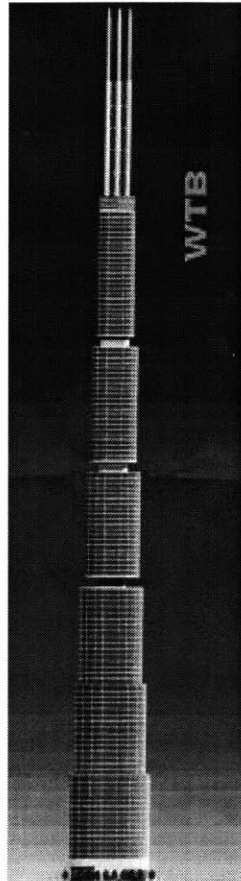
3.3 Torsional Response

Torsional response is the result of the eccentricity resulting from the distance between the center of mass of the building and the center of rigidity of the building. Although varying wind pressure across the face of a building results in some torsional response, the response resulting from inertial forces that are caused by the eccentricity mentioned above dominate. Wind Tunnel tests are the only means of measuring torsional response in buildings.

4.0 Controlling motion in High Rise Structures

4.1 Aerodynamics

7 South Durban Street,
Chicago, Illinois



One Financial Center
Shanghai, China

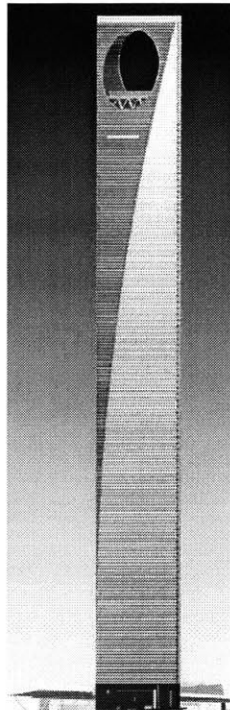


Figure 13 – Aerodynamically Shaped Buildings

The Shape of a building greatly influences the nature of wind loading applied on it. An aerodynamic engineer can spend a lot of time trying to optimize the shape of a building so that the effects of wind are reduced. This type of method of controlling wind loading is very powerful because it is a way of preventing the application of wind load rather than trying to control its effects afterwards.

This method is powerful however, the shape of a building is dictated by Architecture and functionality requirements, which are not usually flexible to reshaping for optimum aerodynamic behavior.

Having said that there are current buildings under consideration, which as part of their architectural characteristics, have included features that allow better performances under wind loading. Figure 13 shows One Financial center proposed in Shanghai, China. This tall building has a large diameter hole at the top of the building. The circular hole allows wind in the boundary layer to pass through the building which reduce the along wind forces and at the same time prevents the separation of the boundary layer thus preventing the creation of alternating vortices.

Figure 13 also shows 7 South Durban Street in Chicago that is currently the tallest building in the world under consideration. This 1588ft tall structure has filleted corners, which serve the purposes of reducing the boundary layer separation that case cause vortex shedding

The building also has notches taken out at certain intervals that serve the purpose of separating the residential complex from the office complex and at the same time, serve the purpose of reducing the effects of boundary layer separation and the effects associated with vortex shedding phenomena.

4.1 *Passive Control*

Passive control means control without the help of an external source of energy. In the case of a building, stiffness and damping are methods of passive control. One adjusts the stiffness and/or damping properties of a building in an effort to limit the motion of the structure. In this section the effects of modifying the damping parameters on the response of a structure is discussed. Different types of devices are introduced that allow the increase of damping in a building.

Damping is the process by which physical systems such as structures dissipate and absorb energy input from external excitation. Damping reduces the build up strain energy especially near resonance conditions where damping governs the response. Damping dissipates energy over a response cycle. For low damping ratio, the energy dissipated per cycle is small and thus many cycles are required before the energy input is eventually dissipated.

Dissipation and absorption are attributed to a number of external and internal mechanisms. Three of the mechanisms are described below.

Energy dissipation due to the viscosity of a material. This process depends of the time rate of deformation.

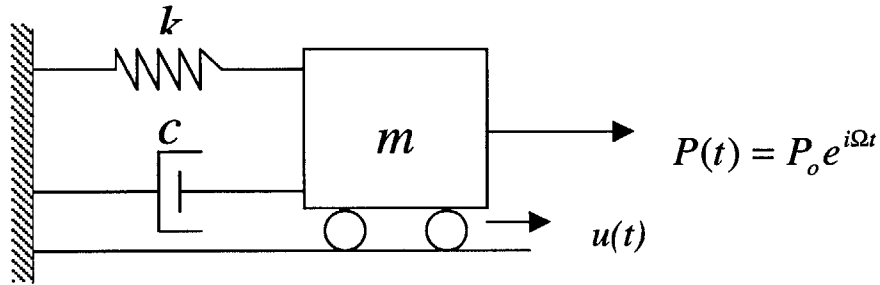
Energy dissipation and absorption caused by the material undergoing cyclic inelastic deformation and ending up with some residual deformation

Energy associated with overcoming friction between moving bodies in contact, such as flexible connections.

Numerous experiments have been conducted to determine the damping ratio of a building, as it is impossible to determine it analytically. The tests indicated that for steel and concrete buildings the critical damping ratio, ξ , is about 0.01.

In design of tall buildings, it is extremely important to know the damping ratio of the building because damping is the only mechanism available to control motion when the frequency of a forcing function is near the natural frequency of the structure.

For the purposes of illustrations, consider a one-degree of freedom system with a spring and a damper;



From dynamics;

$$m\ddot{u} + c\dot{u} + ku = P_o e^{i\Omega t}$$

$$u(\omega) = H_1(\omega) \frac{P_o}{k}$$

where $\frac{P_o}{k}$ is the deflection if the load was static and

$$H_1(\omega) = \frac{1}{\sqrt{\left[1 - \left(\frac{\Omega}{\omega}\right)^2\right]^2 + \left[2\xi \frac{\Omega}{\omega}\right]^2}} \quad \text{is the dynamic amplification factor}$$

Similarly that it can be shown that the acceleration can be expressed as

$$a(\omega) = H_2(\omega) \frac{P_o}{m}$$

$$H_2(\omega) = \frac{\left(\frac{\Omega}{\omega}\right)^4}{\sqrt{\left[1 - \left(\frac{\Omega}{\omega}\right)^2\right]^2 + \left[2\xi \frac{\Omega}{\omega}\right]^2}}$$

It is clear to see from the equations that the magnification factors $H_1(\omega)$ and $H_2(\omega)$ become extremely large when the frequency of the forcing function approaches the natural frequency of the structure. In fact, the only factor that is preventing the magnification factor and thus the response from going to infinity is the presence of the damping ratio.

So it is very important for an engineer designing structures subjected to dynamic loading to be able to modify or specify the damping ratio of a building. How then, is one able to establish the damping ratio of a building that will allow him or her to control motion to a specified limit? Devices are available and have been successfully used in high-rise structures that would allow one to adjust the damping ratio of a building. Before introducing these devices, it is worth discussing the concept behind viscous damping because most damping devices, whether or not they exhibit viscous characteristics in dissipating energy, are treated as equivalent viscous dampers for mathematical convenience.

Viscous damping is defined as the energy dissipating mechanism where the damping force is a function of the time rate of change of displacement.

$$F = f(\dot{u})$$

The linearized form is written as

$$F = c\dot{u}$$

where c is the damping coefficient. The work done by the viscous force in one cycle is given by;

$$W = \int_{t_1}^{t_2} F\dot{u}dt = c\pi\Omega\dot{u}^2$$

A possible design for a viscous damper is shown below;

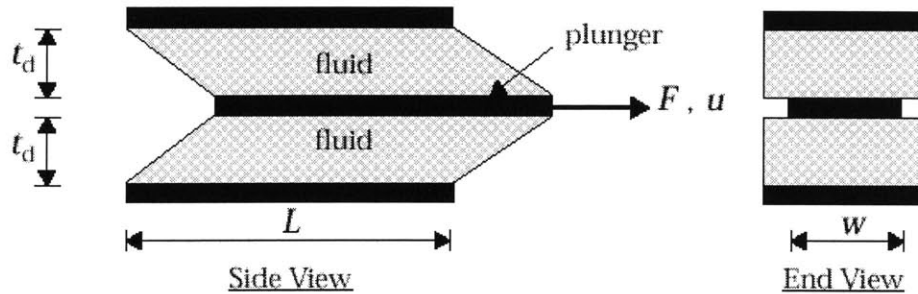


Figure 14- Possible design for a viscous damper

The gap between the plunger and the external plates is filled with linear viscous material characterized by;

$$\tau = G_v \dot{\gamma}$$

where τ = Shearing Stress

$$\gamma = \text{Shearing Strain} = \frac{u}{t_d}$$

The damping force is then equal to

$$F = 2wl\tau$$

Making Substitutions one gets

$$F = \left[\frac{2wlG_v}{t_d} \right] \dot{u}$$

Then

$$c = \left[\frac{2wl}{t_d} \right] G_v$$

one would then calculate ξ from;

$$\xi = \frac{c}{2\sqrt{km}}$$

or as is done in motion-based design, one evaluates c from a desired damping ratio. Such devices are available, and below are pictures of such a device from Taylor Devices.

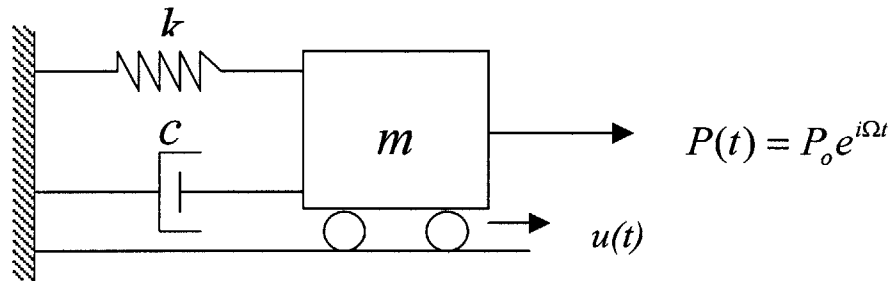


Figure 15 – Fluid Viscous Dampers

Other forms of damping include friction dampers, hysteretic dampers and visco-elastic dampers. Friction dampers absorb energy through friction and the energy dissipated equals the work done by the friction force. Hysteretic dampers dissipate energy through inelastic deformation. Visco-elastic materials exhibit the properties of viscous and elastic materials in their energy absorption mechanism.

As said before, it is mathematically advantageous to express these dampers as equivalent viscous dampers. This is done by equating the work done by each damper to the work done by a linear viscous damper. An equivalent damping coefficient for Coulomb, Structural, Hysteretic and Visco-elastic dampers is given in [8].

To address the question posed earlier on how one can alter the damping ratio of a system to control motion, the following illustration of a single degree of freedom subjected to a harmonic forcing function that has the same frequency as the natural frequency of the system is presented next.



$$\omega = \Omega$$

Let $P_o = 10\text{N}$

$M = 1000\text{kg}$

And the maximum acceleration is to be limited to 0.02

Then $H_2(\omega) = \frac{a(\omega)m}{P_o} = 2$

Then from $2 = \sqrt{\frac{(1)^4}{[1 - (1)^2]^2 + [2\xi 1]^2}}$

Solving For ξ

$$\xi = \frac{1}{4} = 0.25^*$$

Then Calculate c from

$$c = \xi 2\sqrt{km}$$

One would then specify the value of c and the force in the damper to a damper manufacturer and buy the devices shown in Figure 15.

The example shown here is for a single degree of freedom system. The concept is similar in the multi degree of freedom system except that one deals with modal force, modal mass and modal damping ratio. In multi-degree of freedom systems, one usually designs for the fundamental mode and checks the design for higher modes. Damping in multi-degree of freedom structures is presented in [8].

The type of damper to be used depends on the structural system of a building. From the brief description of the structural systems of high-rise buildings presented in chapter two, one can see the applicability of the different types of dampers. Viscoelastic dampers, which are usually made of rubber with steel shims embedded in them, were successfully used in the world trade center building. They were placed between connections. Linear viscous dampers lend themselves for use in building with x-braces. A project around this area that proposes to use linear viscous dampers is the Millennium Place in downtown Boston. Hysteretic Dampers have been used successfully in Asia as braces. Innovative ways of allowing the point at which yielding and buckling occur led to the use in large span braces.

* This value for damping ratio is high. Conventional Steel Buildings have a natural damping ratio of 0.01.

Conclusion

High-Rise structures today are becoming more flexible and the structural engineer is faced with the challenge of developing new approaches to control motion in high-rise structures. Unlike the high-rises of the 1940s, which were designed for strength and checked for serviceability, today's high rises are designed to limit motion and checked to satisfy strength. This shift in design philosophy is happening in all flexible structures including large span bridges.

In order for a structural engineer to implement strategies to control motion in high-rise structures, a full understanding of the nature of wind is required. One also needs to understand the mathematics involved in applying wind loading to structures as well as the results of any wind tunnel tests conducted. That is discussed in the first part of the thesis.

A structural engineer also needs to understand the different structural systems of high-rise structures and the different responses of a structure to dynamic wind loading. It is only after a complete understanding of these properties that one can start to select the method to control motion. The actual selection of control method then depends on the structural system. This is discussed in the second part of the thesis.

Appendix I

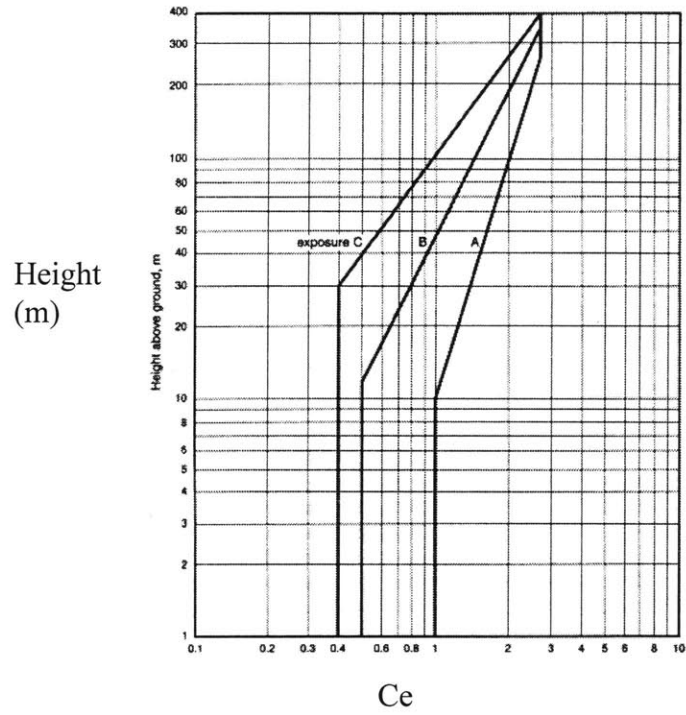


Figure 16 Exposure Factor

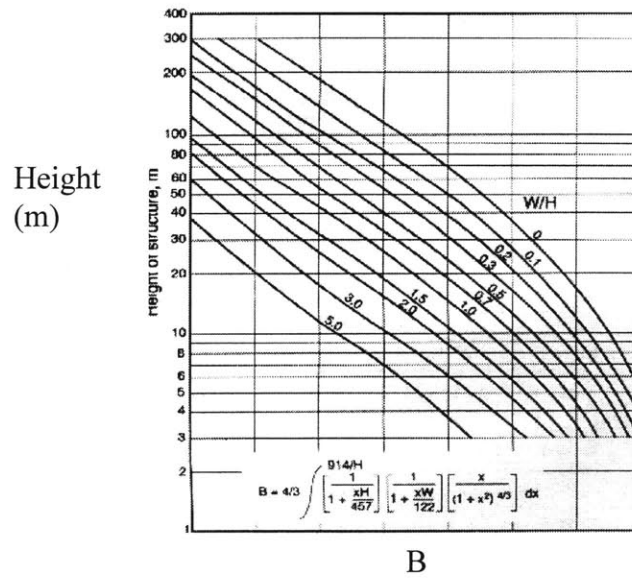


Figure 17 Background Turbulence Factor

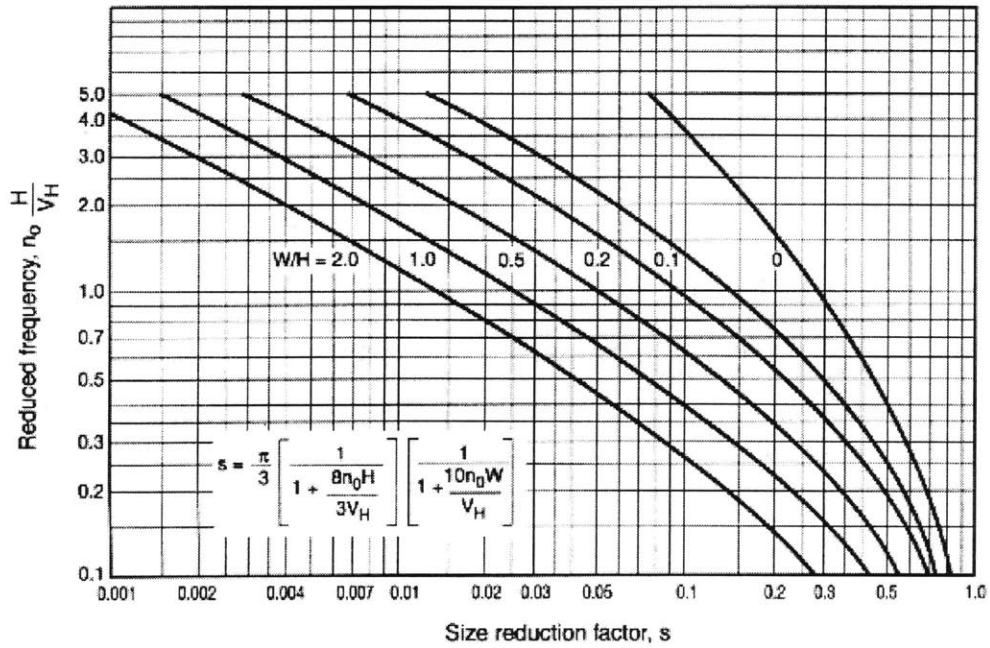


Figure 18 Size Reduction Factor

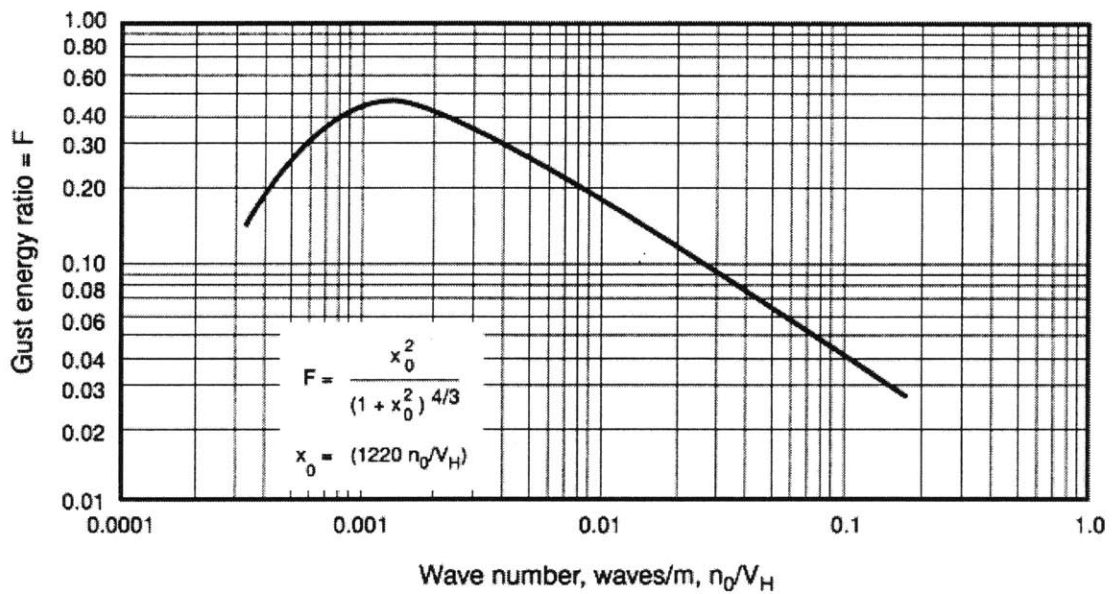


Figure 19 Gust Energy Ratio

Bibliography

- [1] Emil Simiu and Robert H. Scanlan. *Wind Effects on Structures*. John Wiley & Sons, New York, 1996
- [2] Bryan Stafford Smith and Alex Coull. *Tall Building Structures. Analysis and Design*. John Wiley & Sons, New York, 1991
- [3] International Symposium Proceedings. *Wind Load on Structures*. 1991
- [4] Bungale S. Taranath. *Steel, Concrete, and Composite Design of Tall Buildings*. Second Edition. McGraw-Hill, 1998
- [5] Edwin H. Gaylord Jr. and Charles N. Gaylord. *Structural Engineering Handbook*. Third Edition. McGraw-Hill, 1990
- [6] Anil Chopra. *Dynamics of Structures*. Prentice Hall, 1995
- [7] Claes Dyrbye and Svend O. Hansen. *Wind Load on Structures*. John Wiley and Sons, 1997
- [8] Jerome J. Connor and B. S. A Klink. *Introduction to Structural Motion Control*.
- [9] H. Buchholdt, *Structural dynamics for engineers*, Great Britain, 1997
- [10] National Building Code of Canada, 1995, Users guide Structural Commentaries, Part 4